Vol. **114** (2008) *ACTA PHYSICA POLONICA A* No. 5

Proc. XXXVII International School of Semiconducting Compounds, Jaszowiec 2008

Spatially Resolved X-ray Diffraction Technique for Crystallographic Quality Inspection of Semiconductor Microstructures

J.Z. Domagala, A. Czyzak and Z.R. Zytkiewicz*

Institute of Physics, Polish Academy of Sciences
al. Lotników 32/46, 02-668 Warsaw, Poland

Spatially resolved X-ray diffraction is introduced and applied for micro-imaging of strain in GaAs and GaSb layers grown by epitaxial lateral overgrowth on GaAs substrates. We show that laterally overgrown parts of the layers (wings) are tilted towards the underlying mask. By spatially resolved X-ray diffraction mapping the direction of the tilt and distribution of tilt magnitude across the width of each layer can be readily determined. This allows measuring of the shape of the lattice planes in individual epitaxial stripes. In GaSb/GaAs heteroepitaxial laterally overgrown layers local mosaicity in the wing area was found. By spatially resolved X-ray diffraction the size of microblocks and their relative misorientation were analyzed. Finally, microscopic curvature of lattice planes confined between two neighboring slip bands in thermally strained Si wafers is measured. All these examples show advantages of spatially resolved X-ray diffraction over a standard X-ray diffraction when applied for analysis of crystalline microstructures.

PACS numbers: 61.05.cp, 61.72.Ff, 68.55.ag

1. Introduction

As the result of miniaturization of semiconductor devices there is an increasing demand for techniques that allow detection and visualization of μm size crystalline lattice defects. From the many techniques available the X-ray rocking curve imaging (RCI), based on synchrotron X-ray diffraction, has gained much attention recently as a method of wafer defect analysis [1]. However, for most crystal growers laboratory techniques are preferred. Therefore, we have developed a micro-imaging technique based on spatially resolved X-ray diffraction (SRXRD) that makes use of conventional high resolution X-ray diffractometer.

*corresponding author; e-mail: zytkie@ifpan.edu.pl

In order to show advantages of the SRXRD technique over a standard X-ray diffraction when applied for analysis of crystalline microstructures three examples will be presented in this report. First, we focus on SRXRD studies of epitaxial laterally overgrown (ELO) GaAs layers grown by liquid phase epitaxy (LPE) on SiO_2-masked GaAs substrates. ELO layer consists of a few hundreds micrometers wide monocrystalline stripes regularly arranged on a substrate. Since each stripe is strained such samples contain a periodic distribution of strain and/or defects. Thus, they are very suitable to demonstrate potential of the technique. High spatial and angular resolutions of SRXRD allow studying an effect of ELO wings tilt towards the mask. Direction of the tilt and the distribution of tilt magnitude across width of each wing were determined. Then we switch to heteroepitaxial GaSb/GaAs ELO layers, in which a local mosaicity in the wing area is found. By SRXRD the size of microblocks and their relative misorientation were analyzed. As the final example, we report on strain distribution in thermally strained Si wafers.

2. Idea of SRXRD and experimental details

High resolution X-ray diffraction is commonly used for structural analysis of crystalline samples. Usually the rocking curves (RC) and reciprocal space maps are measured. In standard diffractometers a typical size of X-ray beam cross-section is in the range of 1 cm^2. This leads to a highly intensive diffracted beam and to high signal/noise ratio. Under such conditions, however, the signal obtained is integrated over a large sample area, so information on local lattice distortion is difficult to extract. Therefore, we implemented the SRXRD technique as presented schematically in Fig. 1: the incident X-ray beam is reduced by set of slits to a desirable size and its position stays fixed. The longer side of X-ray beam is parallel to the direction of seeding lines. Then, ω or $2\theta/\omega$ scans are recorded in double or triple axis geometry from precisely defined area of the sample. Then, the sample is moved in direction perpendicular to the seeding lines in very small steps and new measurements are taken. Finally, all the curves are collected to create an X-ray image (X-ray map) of the area studied. Historically, the technique originates from our earlier local XRD experiments [2]. Then, it evolved into its final version with complete mapping capabilities (see [3, 4] for more details).

Phillips X'Pert MRD X-ray diffractometer equipped with a fourfold Ge (220) monochromator, a threefold Ge (220) analyzer, and an X-ray mirror was used for SRXRD experiments. In its standard version the diffractometer produces 12 mm high and 1 mm wide X-ray beam. Typical intensity of 004 reflection from GaAs sample is a few 10^6 count per second (cps) in double axis geometry if the X-ray tube with a copper anode (maximum power of 2.2 kW) is used. With our detection limit of a few hundreds cps the system allows examination of objects having dimensions larger than $10/\sin\theta_B \times 100\ \mu m^2$, where θ_B is the Bragg angle of the reflection studied. For the 004 reflection of GaAs this corresponds to a spatial resolution of $18 \times 100\ \mu m^2$.

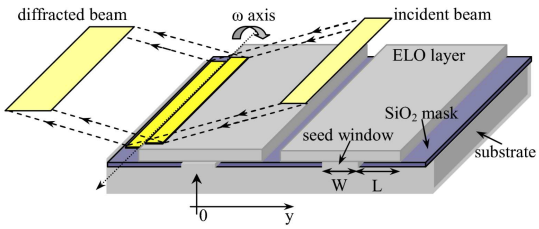

Fig. 1. Geometry of SRXRD measurement of ELO structure; y marks position of the beam on the sample, ω is the axis of sample rotation during the ω scan.

3. Results and discussion

3.1. GaAs:Si/GaAs ELO layers

The Si-doped GaAs ELO layer studied in this work was grown by LPE on undoped (001) GaAs substrate coated by 0.1 μm thick SiO_2 mask. Details of the growth procedure can be found elsewhere [5]. The layer consisted of separated, ≈ 300 μm wide GaAs stripes grown from 10 μm wide line seeds (windows) opened in the mask. The windows were oriented 15° off from the $\langle 001 \rangle$ direction. For the purpose of this work only a single GaAs stripe was examined while the rest of the sample was covered with a Pb foil. Plane view of the sample is shown in Fig. 2a.

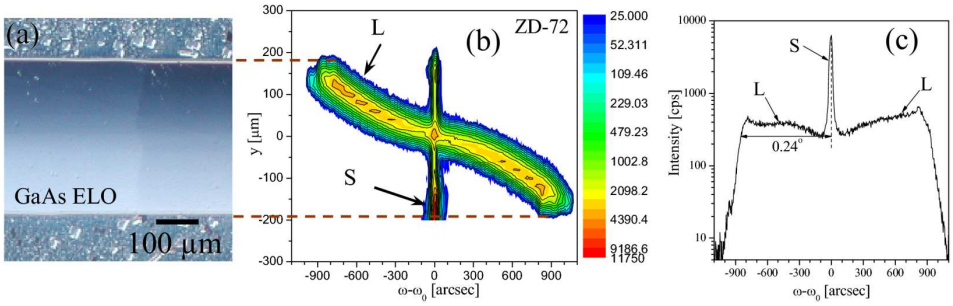

Fig. 2. Plane view of a single GaAs ELO stripe (a) and RC map of the sample (b); standard wide beam RC is shown in (c). "S" and "L" mark signals from the substrate and the layer, respectively.

Figure 2b presents an experimental RC map of the GaAs ELO stripe measured without an analyzer. The X-ray beam size was 10 μm $\times$ 10 mm and the sample was moved in direction perpendicular to the seed line in steps of 20 μm in the range of ± 200 μm to analyze the whole width of the stripe. The map is plotted in coordinates (y) and $(\omega - \omega_0)$, where y marks position of the beam on the sample and ω_0 denotes the Bragg angle of the substrate (Fig. 1). There are two signals clearly seen on the map. The first one marked as "S" comes from the GaAs substrate. Its position on the map does not change, which indicates that substrate (001) lattice planes are not deformed. The second signal marked as "L"

originates from Si doped GaAs ELO layer. Its angular position $\alpha(y) = \omega(y) - \omega_0$ changes continuously from 0.24° to -0.24° when the beam spot moves from the left to the right edge of the ELO stripe. A simple geometrical analysis shows that such shape of the map indicates downward bending of the (001) lattice planes of the layer [4]. For an upward lattice bending the RC map would be a mirror reflection of the image shown in Fig. 2b relative to the $\omega = \omega_0$ line.

Downward tilt of lattice planes, being due to an interaction between ELO wings and the mask, is a well known phenomenon commonly observed in various ELO systems, including ELO layers of GaAs [2] and Si [6] grown by LPE as well as GaN ELO layers grown by metalorganic vapor phase epitaxy [7]. When studied by standard wide beam X-ray diffraction the effect manifests itself by broadening of X-ray rocking curve measured with the axis parallel to the seeding line (see Fig. 2c). Actually, a half width of such curve is a good measure of the wing tilt angle [2]. It should be noted, however, that upward and downward tilts cannot be distinguished from the standard X-ray rocking curve and additional experiments, e.g. local electron diffraction [8], must be used to determine the wing tilt direction. On the contrary, the SRXRD experiment provides much more information. As mentioned already, shape of the RC map in Fig. 2b indicates unambiguously wing tilt direction. Angular position $\alpha(y)$ of the ELO signal gives distribution of the local tilt angle across the GaAs stripe. In particular, the tilt of 0.24° at the edge of ELO wing can be found from Fig. 2b in agreement with the standard XRD experiment (Fig. 2c). By measuring the tilt angle distribution the shape of bent (001) lattice planes can be calculated since a local displacement $h(y)$ of lattice planes is proportional to $\partial\alpha/\partial y$ [4]. Moreover, the width of the GaAs stripe (≈ 302 μm) can be determined from the RC map by measuring the spatial spread of the ELO signal. Finally, dispersion of wing tilt can be studied if large area containing many ELO stripes or fully overgrown ELO structure is mapped [9]. In that way the high spatial resolution offered by SRXRD makes the technique a powerful tool to study local lattice distortions in semiconductor microstructures.

3.2. GaSb:Si/GaAs ELO layers

Figure 3a shows plane view of Si-doped GaSb ELO stripe studied in this work. The sample was grown by LPE on undoped (001) GaAs substrate covered by 2 μm thick planar GaSb buffer and by 0.1 μm thick SiO_2 mask with 10 μm wide seeding line openings. Surface of the sample has been etched to reveal distribution of dislocation pits. As seen, dislocations generated due to lattice mismatch between the GaSb buffer with the substrate emerge on the GaSb ELO surface in the central part of the layer just above the opening in the mask, while the whole rest of the layer is very homogeneous and nearly dislocation free. This is a direct proof of highly efficient filtration of dislocations in ELO procedure [10]. However, despite a good confinement of threading dislocations and a smooth surface morphology, the X-ray RC obtained with the beam wider than the ELO stripe (standard XRD

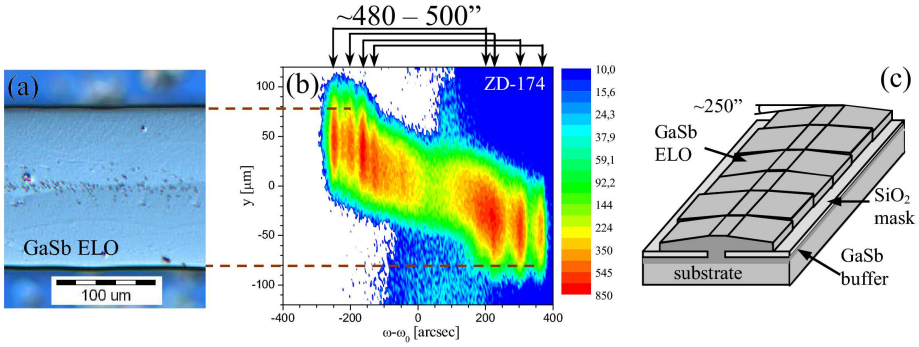

Fig. 3. Plane view of GaSb/GaAs ELO layer after its etching to reveal dislocation pits distribution (a) and RC map of the sample measured with an analyzer (b); structure of GaSb microblocks is shown schematically in (c).

— not shown) is quite broad and contains a few maxima. In order to explain their origin the layer was studied with the use of SRXRD technique.

Figure 3b shows RC map of the GaSb stripe measured with the 10 μm $\times$ 10 mm X-ray beam and the sample movement step of 3.5 μm. Symmetrical GaSb 004 reflection was used in the experiment. Moreover, an analyzer adjusted to the Bragg angle of the Si-doped GaSb ELO layer was applied to extract only the signal from the ELO stripe. In general, shape of SRXRD map of the layer is similar to that of GaAs ELO layer. As before, this indicates tilting of ELO wings towards the mask. Let us note however that in Fig. 2b the local tilt magnitude $\alpha(y) = \omega(y) - \omega_0$ varies continuously with y, whereas the map of the GaSb/GaAs sample contains pairs of discrete streaks located at fixed angular positions. Such shape of the map indicates microstructure of the GaSb layer as shown in Fig. 3c: the ELO layer consists of microblocks, inside which the ELO wings are flat, but tilted towards the mask. Then, the RC image of the single microblock should have a shape of a pair of streaks, angular separation of which on the map ($\approx$ 480$-$500 arcsec) equals to misorientation of ELO wings. Basing on independent XRD experiments we have estimated the typical size of the microblock in the direction of the seeding line as equal to $\approx$ 100 μm. Moreover, these microblocks are tilted relative to each other in the plane perpendicular to the seeding line direction. Since the length of the X-ray beam along the seed direction is much larger, many microblocks contribute simultaneously to diffracted signal and the RC map contains a series of shifted streaks. Thus, the relative misorientation of GaSb microblocks of $\approx$ 40 arcsec can be concluded from Fig. 3b. It is worth mentioning that despite relative misorientation of GaSb microblocks the wing tilt inside them seems to be the same ($\approx$ 240$-$250 arcsec). Since the mask induced wing tilt takes place during ELO growth [11] this might indicate that the layer grew at high temperature without any mosaic structure and the mosaicity was created during post growth cooling to accommodate thermal strain

in the ELO structure. Let us note also that boundaries between the microblocks are not revealed by selective etching (Fig. 3a). This means that there is negligible number of strain relieving defects at these boundaries and the respective strain there is elastic.

3.3. Thermally strained Si wafers

As the final example we report on application of the SRXRD microimaging technique for studying lattice planes deformation in thermally strained saddle--shaped Si (001) wafers. Figure 4a shows a defect that is sometimes observed at edges of Si wafers when they experience a large thermal stress, e.g. during high temperature annealing or epitaxial growth. The defect consists of a pair of neighboring slip bands marked as S_1 and S_2 and separated by a distance of about 1 mm.

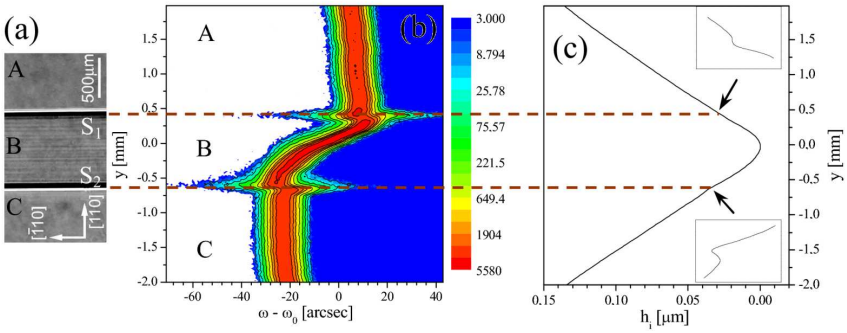

Fig. 4. Plane view of Si wafer with two slip bands S_1 and S_2 (a), RC map of the sample (b) and calculated shape of (001) lattice planes (c).

Figure 4b shows 004 reflection RC map of the Si sample measured with the 10×100 μm^2 X-ray beam having its shorter side parallel to the [110] direction. The sample was moved in steps of 20 μm in the direction perpendicular to the slip band. As seen, angular position of the signal does not change in the areas marked as A and C in Fig. 4a, which means that the Si lattice planes are not deformed there. However, some significant upward lattice plane bending is found just in between the slip bands. Figure 4c shows calculated shape of Si lattice plane along the [110] direction. As expected from the map we found that the (001) lattice plane curvature is locally confined between two neighboring slip bands, with the rotation axis parallel to the slip bands. From the misorientation angle between the two flat regions, the calculated radius of the local curvature is as small as 7 m, indicating that the concave curvature was formed with significant strain localization between the two slip bands. This finding, when correlated with results of independent studies by X-ray topography and transmission electron microscopy, allowed clarifying microscopic structure of dislocations involved in relaxation of strain associated with the thermal processing of Si wafers. In particular, fragmented dislocation

structure was found while the local confinement of plastic deformation was attributed to the multiplication of the dislocations that are generated between the two slip bands [12].

4. Summary and conclusions

Spatially resolved X-ray diffraction technique was used to analyze crystallographic quality of semiconductor microstructures. In homoepitaxial GaAs/GaAs ELO layers tilt of ELO wings was found. Direction of the tilt and the distribution of magnitude across wing area were determined. In heteroepitaxial GaSb/GaAs ELO layers local mosaicity in the wing area was detected. By SRXRD the size of microblocks and their relative misorientation were analyzed. Finally, we reported on strain distribution in thermally strained Si wafers. Microscopic curvature of lattice planes confined between two neighboring slip bands was measured allowing its correlation with the dislocation structure. We showed that all the phenomena presented are difficult to study by standard X-ray diffraction. On the contrary, due to its high spatial resolution the SRXRD technique allows deeper insight into localized strain fields present in semiconductor microstructures.

References

[1] D. Lubbert, T. Baumbach, J. Hartwig, E. Boller, E. Pernot, *Nucl. Instrum. Methods Phys. Res. B* **160**, 521 (2000).

[2] Z.R. Zytkiewicz, J. Domagala, D. Dobosz, J. Bak-Misiuk, *J. Appl. Phys.* **86**, 1965 (1999).

[3] J.Z. Domagala, A. Czyzak, Z.R. Zytkiewicz, *Appl. Phys. Lett.* **90**, 241904 (2007).

[4] A. Czyzak, J.Z. Domagala, G. Maciejewski, Z.R. Zytkiewicz, *Appl. Phys. A* **91**, 601 (2008).

[5] Z.R. Zytkiewicz, *Cryst. Res. Technol.* **34**, 573 (1999).

[6] H. Raidt, R. Kohler, F. Banhart, B. Jenichen, A. Gutjahr, M. Konuma, I. Silier, E. Bauser, *J. Appl. Phys.* **80**, 4101 (1996).

[7] P. Fini, H. Marchand, J.P. Ibbetson, S.P. DenBaars, U.K. Mishra, J.S. Speck, *J. Cryst. Growth* **209**, 581 (2000).

[8] I.H. Kim, C. Sone, O.H. Nam, Y.J. Park, T. Kim, *Appl. Phys. Lett.* **75**, 4109 (1999).

[9] A. Czyzak, J.Z. Domagala, Z.R. Zytkiewicz, *Appl. Phys. A* **91**, 609 (2008).

[10] Z.R. Zytkiewicz, *Thin Solid Films* **412**, 64 (2002).

[11] P. Fini, A. Munkholm, C. Thompson, G.B. Stephenson, J.A. Eastman, M.V. Ramana Murty, O. Auciello, L. Zhao, S.P. DenBaars, J.S. Speck, *Appl. Phys. Lett.* **76**, 3893 (2000).

[12] J.M. Yi, Y.S. Chu, T.S. Argunova, J.Z. Domagala, J.H. Je, *J. Synchrotron Rad.* **15**, 96 (2008).